Supplementary Information

Isolating Hydrogen from Oxygen in Photocatalytic Water Splitting with Carbon-Quantum-Dot/Carbon-Nitride Hybrid

Xijun Wang,[a] Xiang Jiang,[bc] Edward Sharman,[d] Li Yang,[a] Xiyu Li,[a] Guozhen Zhang,[a] Jin Zhao,[bc] Yi Luo,[ac] Jun Jiang*[a]

[a]Hefei National Laboratory for Physical Sciences at the Microscale, Collaborative Innovation Center of Chemistry for Energy Materials, CAS Center for Excellence in Nanoscience, School of Chemistry and Materials Science, University of Science and Technology of China, Hefei, Anhui 230026, P. R. China. *E-mail: jiangj1@ustc.edu.cn

[b]ICQD/Hefei National Laboratory for Physical Sciences at the Microscale, and Key Laboratory of Strongly-Coupled Quantum Matter Physics, Chinese Academy of Sciences, and Department of Physics, University of Science and Technology of China, Hefei, Anhui 230026, China.

[c]Synergetic Innovation Center of Quantum Information & Quantum Physics, University of Science and Technology of China, Hefei, Anhui 230026, China.

[d]Department of Neurology, University of California, Irvine, California 92697, USA

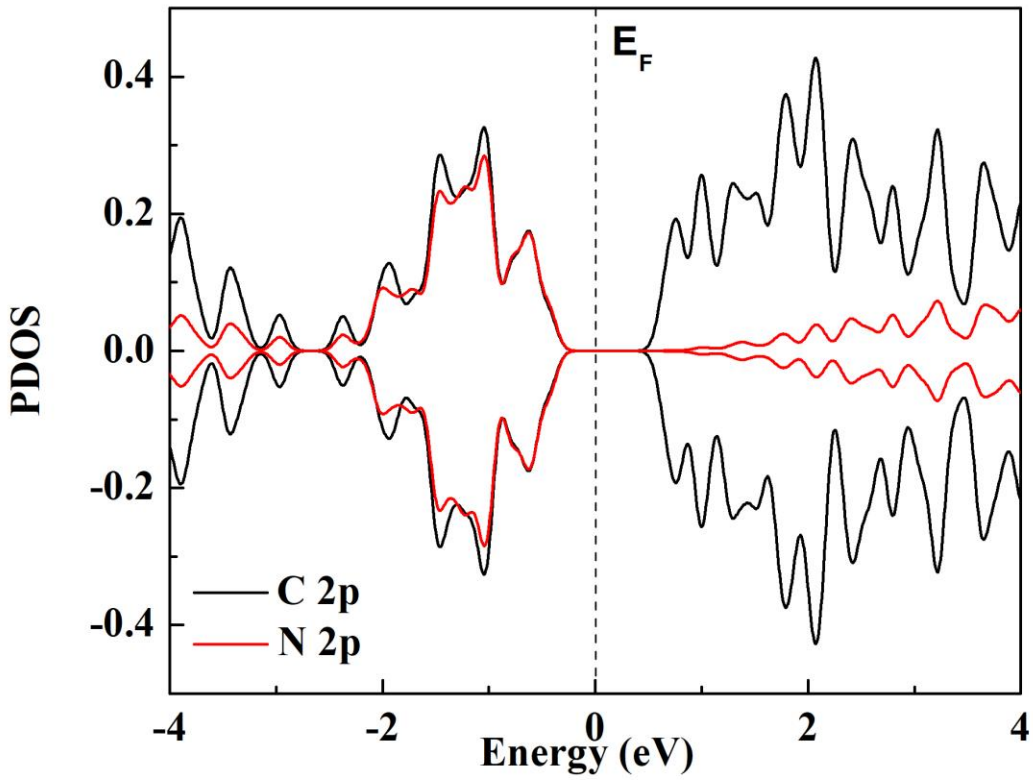

Fig. S1 Computed PDOS of pristine C_3N. Fermi level is set to zero.

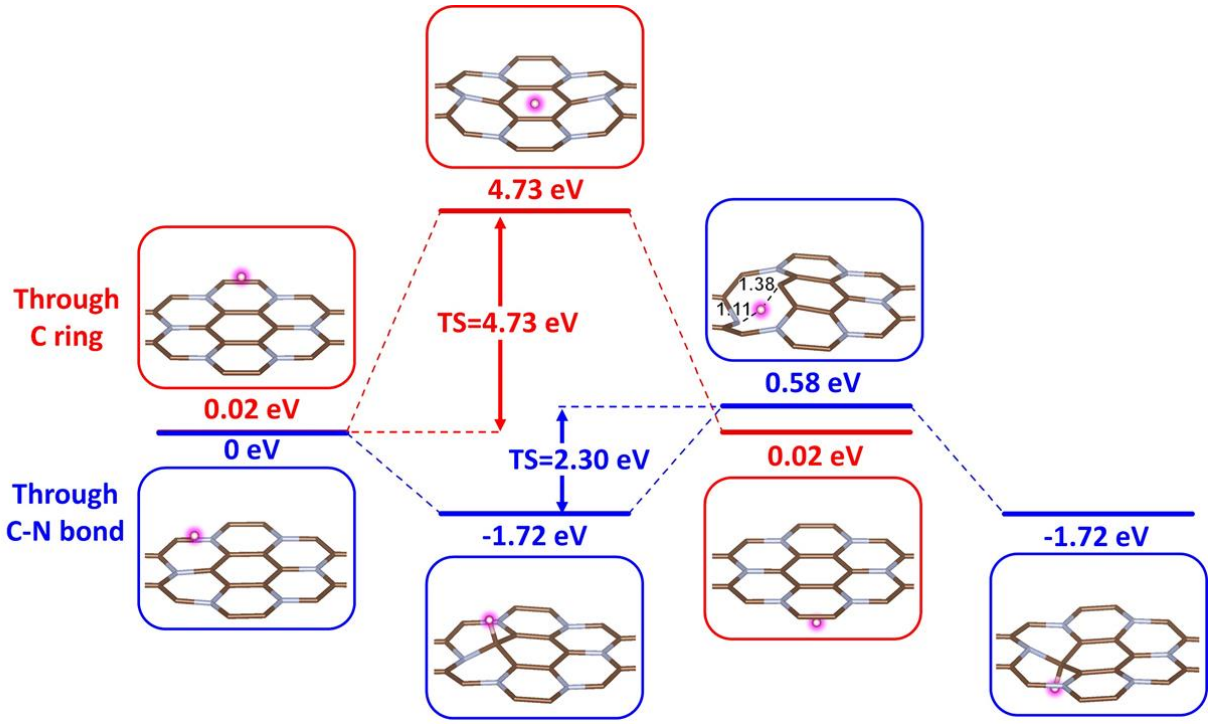

Fig. S2 Energy potential profile along the reaction coordinate for proton migration through the C ring and C-N bond respectively.

The penetration barrier through the C ring (4.73 eV) is much higher than through the C-N bond (2.30 eV).

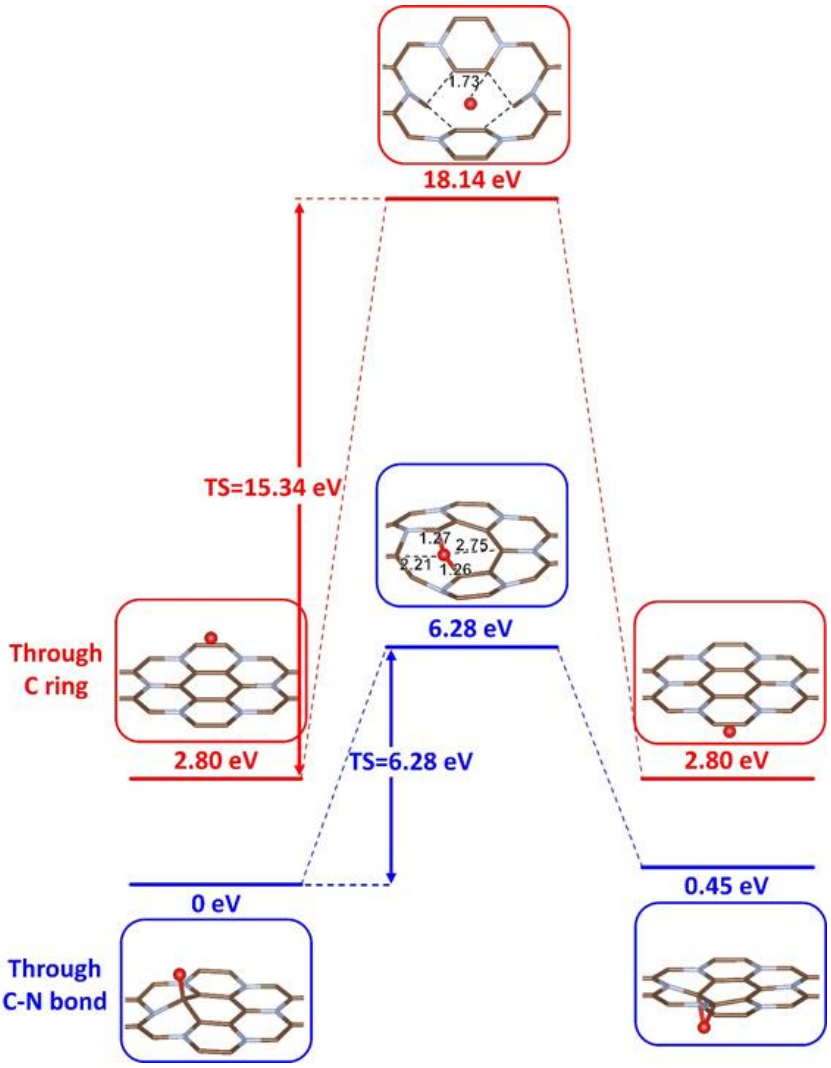

Fig. S3 Energy potential profile along the reaction coordinate for oxygen atom migration through the C ring and C-N bond respectively.

The penetration barrier through the C ring (15.34 eV) is much higher than through the C-N bond (6.28 eV), and both are substantially higher than similar barriers for protons.

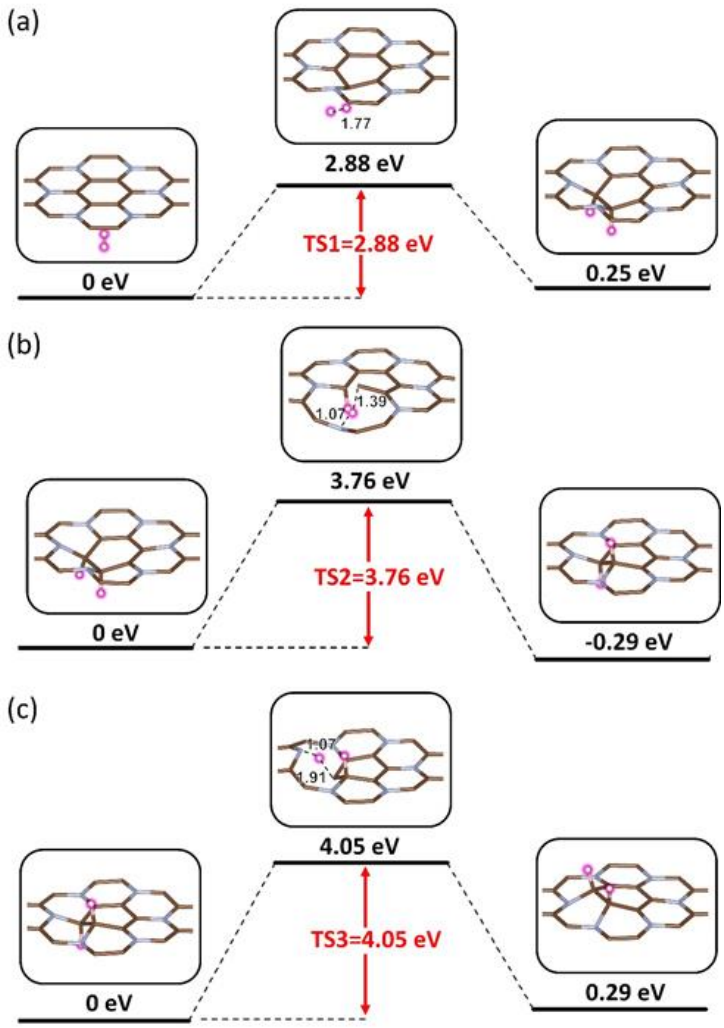

Fig. S4 Energy potential profile along the reaction coordinate for (a) hydrogen molecule splitting, (b) one atomic hydrogen migration and (c) another atomic hydrogen migration through the C_3N layer.

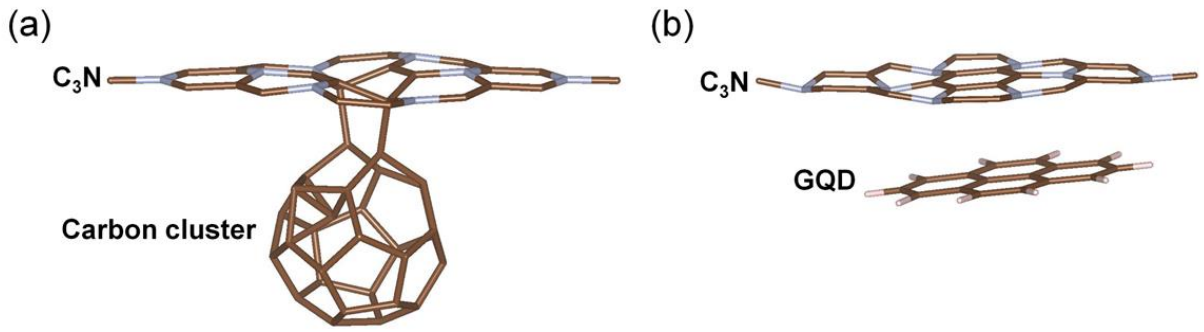

Fig. S5 Alternatives to CQDs: Model of (a) carbon cluster/C_3N and (b) GQD/C_3N configurations.

Table S1. Computed binding energies of carbon cluster/C_3N, GQD/C_3N and diamond (111)/C_3N models.

	Carbon cluster/C_3N	**GQD/C_3N**	**Diamond (111)/C_3N**
Binding energy (eV)	2.52	0.86	0.63

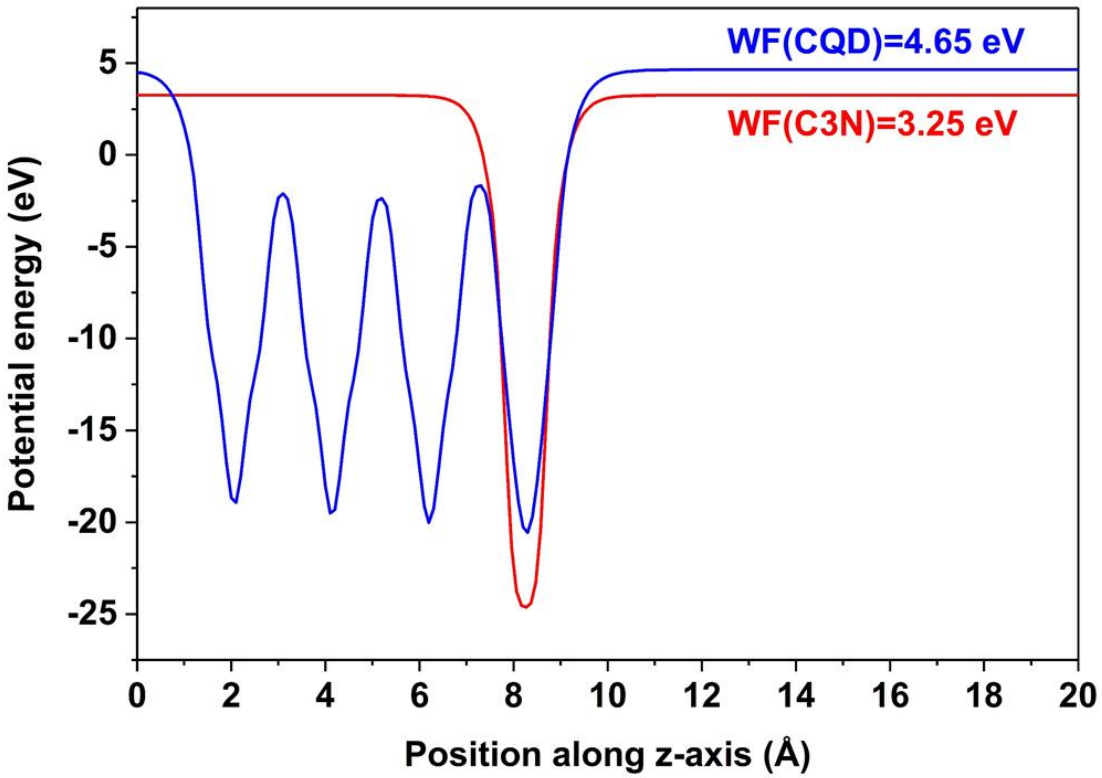

Fig. S6 Potential energy surfaces of bare C_3N (red) and a CQD (blue) along the z-axis. Work functions are the convergent values of these curves.

The work function of C_3N is smaller than that of a CQD, suggesting that electrons should flow from C_3N to CQD, while holes should accumulate on C_3N.

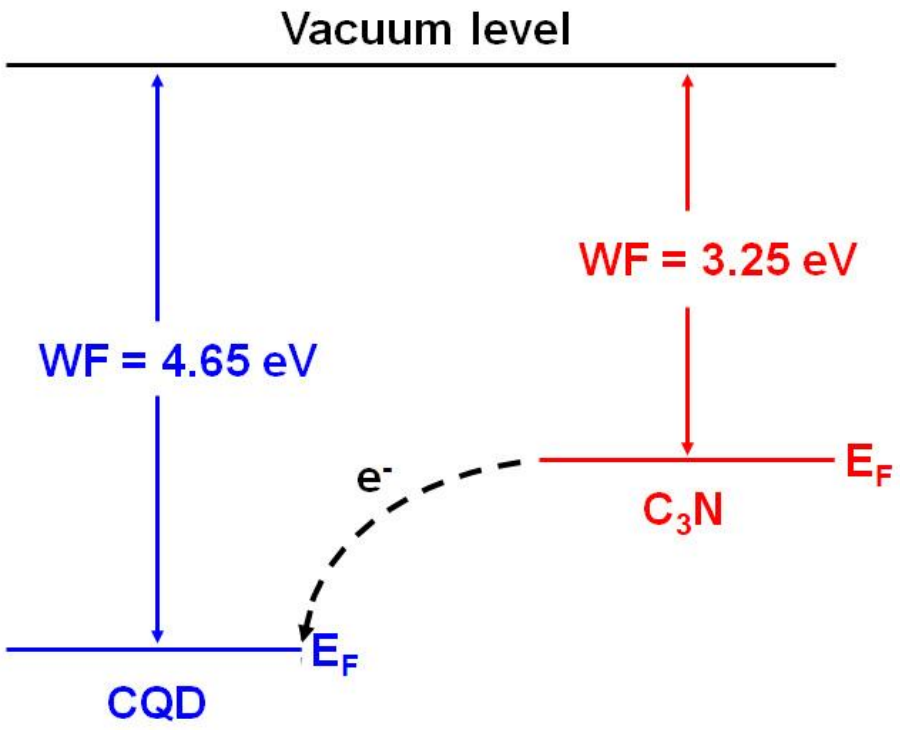

Fig. S7 Schematic illustration of the charge transfer mechanism driven by the work function difference between CQD and C_3N.

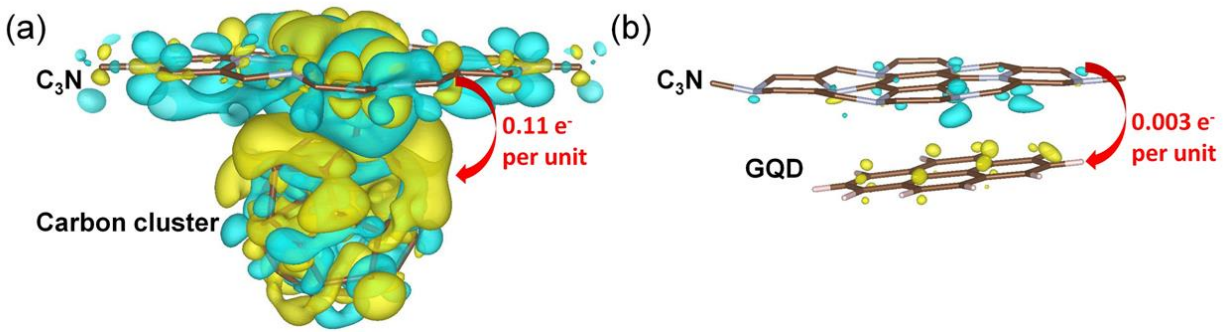

Fig. S8 Charge density differences of the carbon cluster/C_3N and GQD/C_3N structures before light excitation. Yellow and blue bubbles represent electron and hole charge distributions with isosurface values of 0.002 and 0.00025 e/Å^3 respectively.

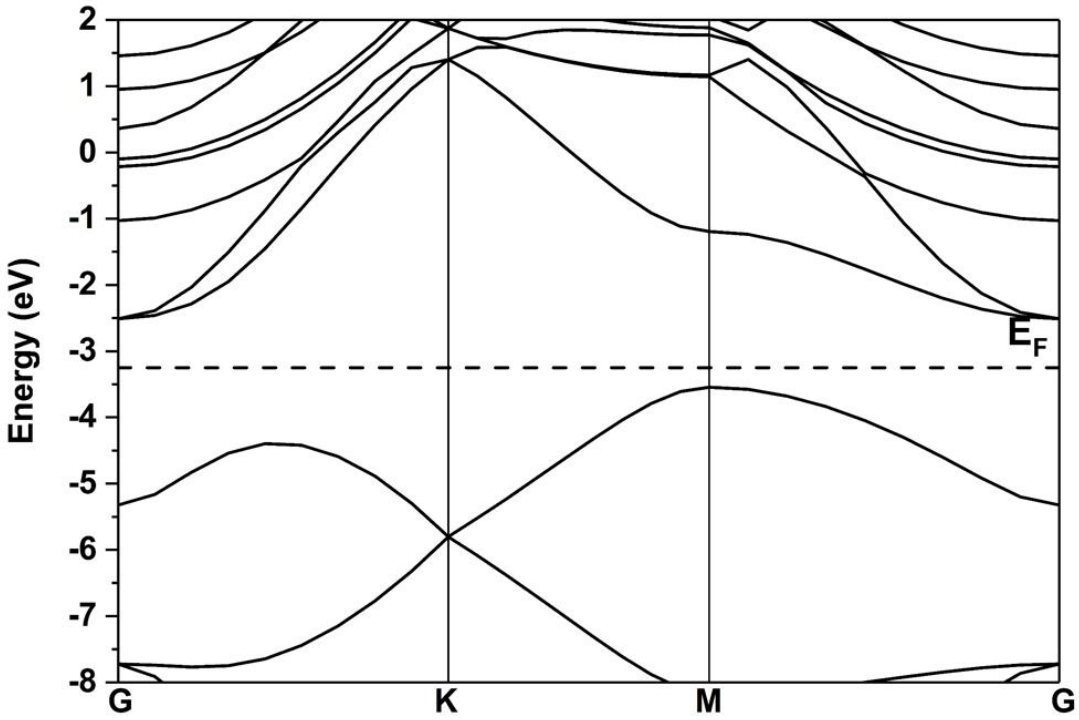

Fig. S9 The computed energy band structure of bare C_3N. G, K, and M represent coordinates for points of high symmetry.

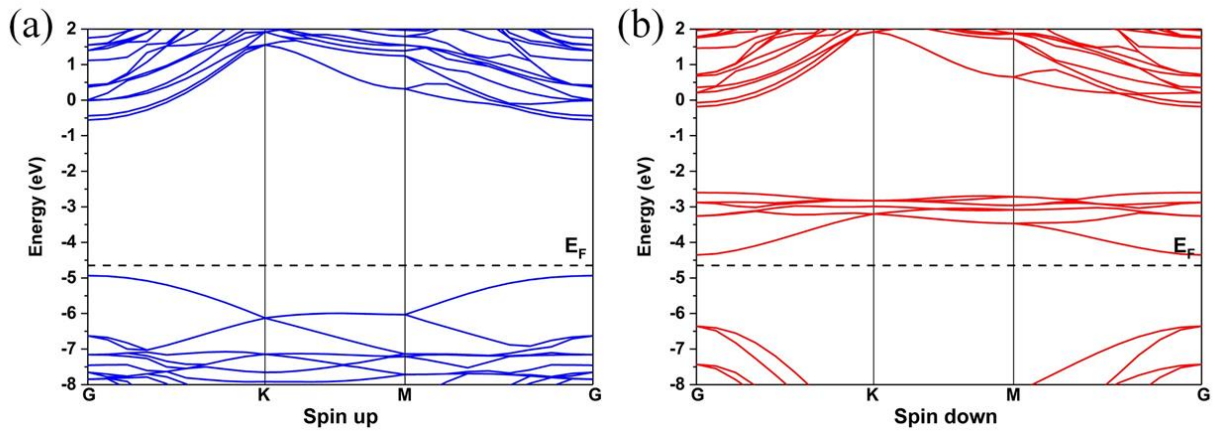

Fig. S10 The computed (a) spin up and (b) spin down energy band structures of bare CQD.

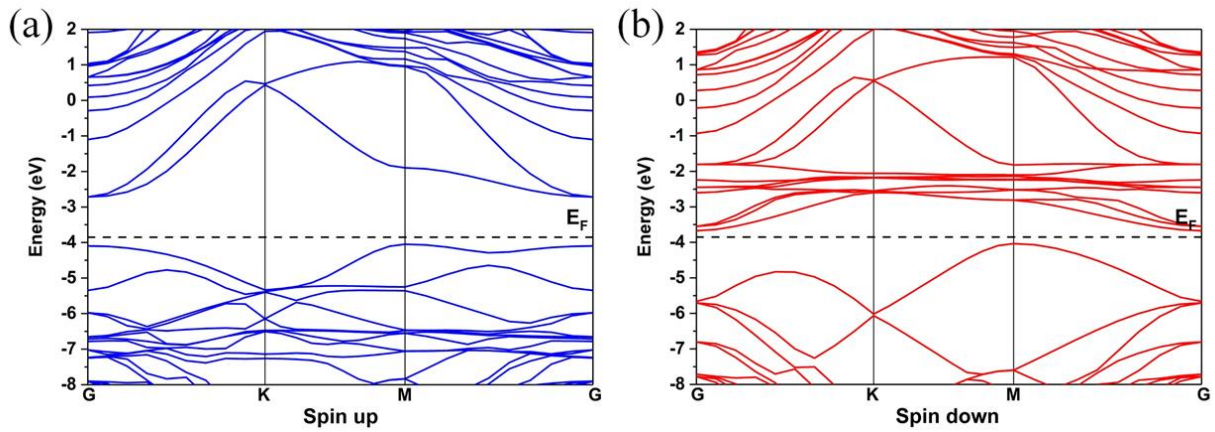

Fig. S11 The computed (a) spin up and (b) spin down energy band structures of the CQD/C_3N composite.

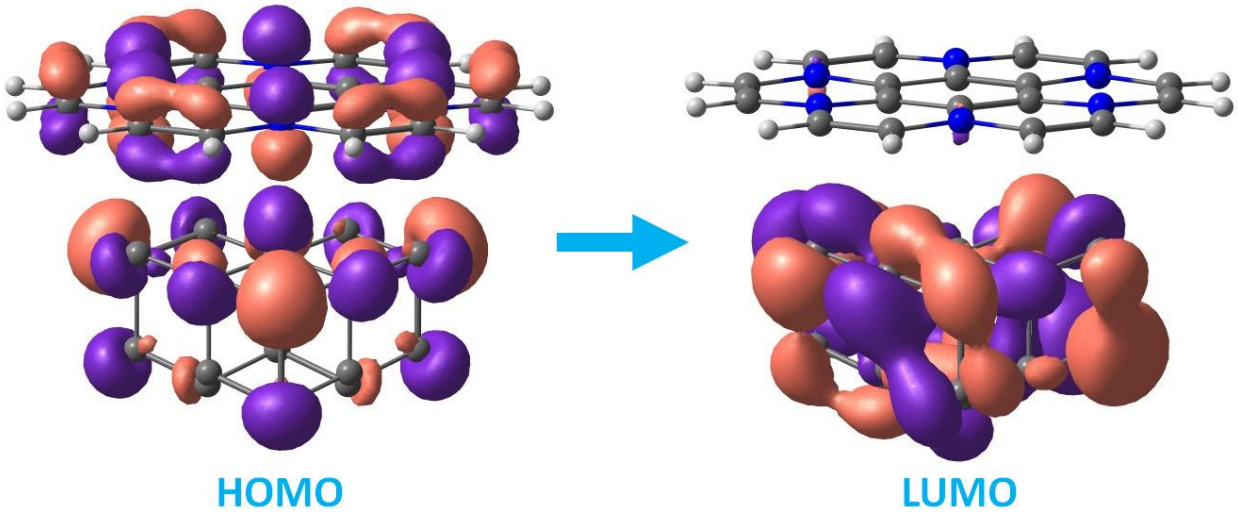

Fig. S12 Highest occupied molecular orbital (HOMO) and lowest unoccupied molecular orbital (LUMO) of CQD/C_3N hybrid computed by PBE functional[S1] and 6-31G basis set[S2] implemented by using Gaussian 16.[S3]

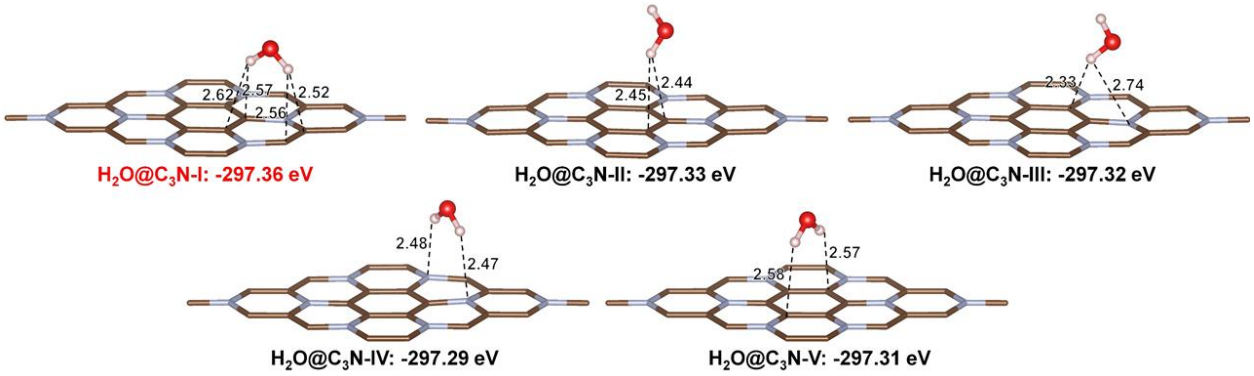

Fig. S13 Various water adsorption configurations on C_3N and their corresponding energies. The most stable one (highlighted in red) was chosen as the initial structure for the subsequent NEB calculations.

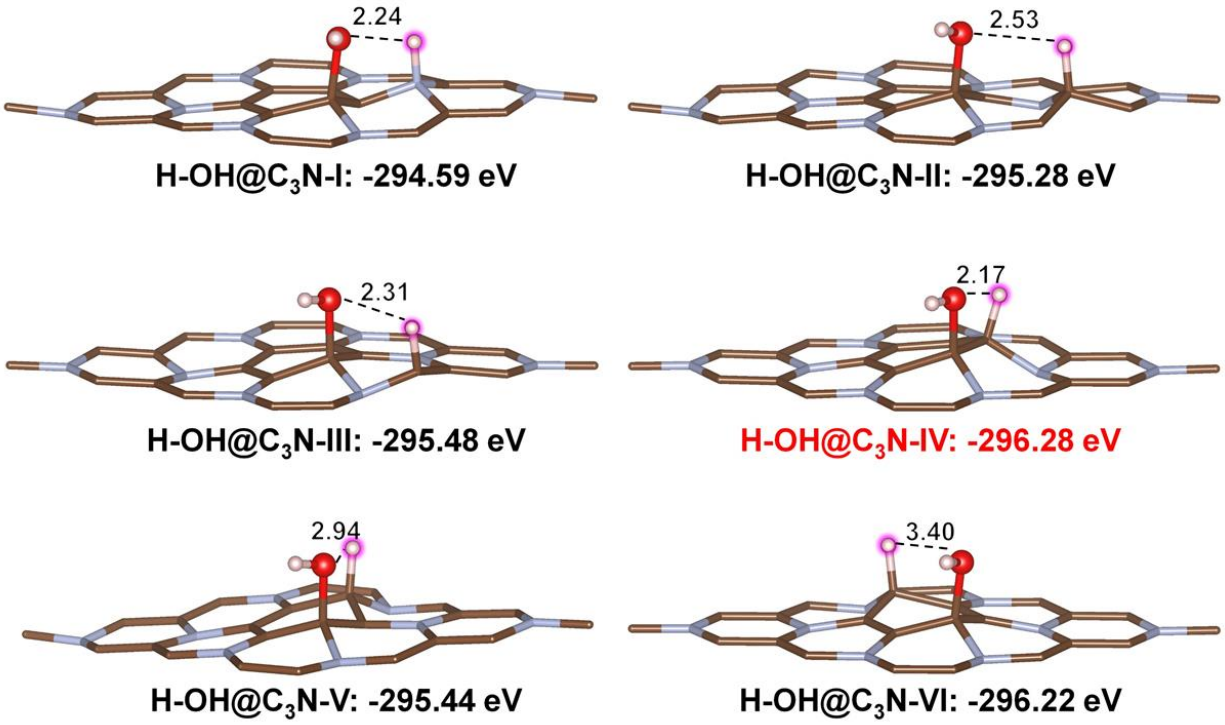

Fig. S14 Various configurations of the products of water splitting on C_3N and their corresponding energies. The most stable one (highlighted in red) was chosen as the final structure for the subsequent NEB calculations.

References

S1. J. P. Perdew, K. Burke and M. Ernzerhof, *Phys. Rev. Lett.*, 1996, **77**, 3865.

S2. V. A. Rassolov, M. A. Ratner, J. A. Pople, P. C. Redfern, L. A. Curtiss, *J. Comput. Chem.*, 2001, **22** (9), 976-984.

S3. M. J. Frisch, G. W. Trucks, H. B. Schlegel, G. E. Scuseria, M. A. Robb, J. R. Cheeseman, G. Scalmani, V. Barone, G. A. Petersson, H. Nakatsuji, X. Li, Gaussian 16, revision A. 03. Gaussian Inc., Wallingford CT. 2016.